Molecular Imaging
Volume 17: 1-9
© The Author(s) 2018
Reprints and permission:
sagepub.com/journalsPermissions.nav
DOI: 10.1177/1536012117749726
journals.sagepub.com/home/mix
SAGE

Reversible Electroporation–Mediated Liposomal Doxorubicin Delivery to Tumors Can Be Monitored With ^{89}Zr-Labeled Reporter Nanoparticles

Govindarajan Srimathveeravalli, PhD[1,2], Dalya Abdel-Atti, BS[1], Carlos Pérez-Medina, PhD[3], Haruyuki Takaki, MD, PhD[4], Stephen B. Solomon, MD[1,2], Willem J. M. Mulder, PhD[3,5], and Thomas Reiner, PhD[1,2]

Abstract

Reversible electroporation (RE) can facilitate nanoparticle delivery to tumors through direct transfection and from changes in vascular permeability. We investigated a radiolabeled liposomal nanoparticle (^{89}Zr-NRep) for monitoring RE-mediated liposomal doxorubicin (DOX) delivery in mouse tumors. Intravenously delivered ^{89}Zr-NRep allowed positron emission tomography imaging of electroporation-mediated nanoparticle uptake. The relative order of ^{89}Zr-NRep injection and electroporation did not result in significantly different overall tumor uptake, suggesting direct transfection and vascular permeability can independently mediate deposition of ^{89}Zr-NRep in tumors. ^{89}Zr-NRep and DOX uptake correlated well in both electroporated and control tumors at all experimental time points. Electroporation accelerated ^{89}Zr-NRep and DOX deposition into tumors and increased DOX dosing. Reversible electroporation–related vascular effects seem to play an important role in nanoparticle delivery to tumors and drug uptake can be quantified with ^{89}Zr-NRep.

Keywords

animal PET, drug delivery, nanoparticle

Introduction

Transient permeabilization of the cell membrane with electric pulses is termed reversible electroporation (RE). Reversible electroporation is used in the preclinical setting and in patients to facilitate the delivery of genetic material and drugs into cells.[1] The pores created in the cell membrane during RE are large enough to admit plasmid,[2] contrast agents,[3] or nanoparticles[4] into the cell. Changes in vascular permeability is a secondary effect of RE and has been reported to elicit a variety of physiologic effects such as transient vascular lock,[5] increased extravasation of large molecules or dyes[6–7] into the surrounding tissue, and the rounding of endothelial layers.[8–9] These 2 features make RE an attractive platform for enhancing the delivery of nanoparticle therapeutics into tumors. Although preliminary experiments combining RE with intra-arterial administration of super paramagnetic iron oxide (SPIO) nanoparticles have demonstrated increased nanoparticle accumulation in RE-treated liver tumors,[10–13] a number of key considerations have to be addressed before this technique can be translated for future patient use.

Preliminary studies evaluating RE for nanoparticle delivery into tumors have focused on membrane permeabilization, and the relative contribution of RE-induced changes in vascular permeability on nanoparticle deposition is not known. The enhanced permeability and retention (EPR) effect observed in

[1] Department of Radiology, Memorial Sloan Kettering Cancer Center, New York, NY, USA
[2] Department of Radiology, Weill-Cornell Medical College, New York, NY, USA
[3] Translational and Molecular Imaging Institute, Department of Radiology, Icahn School of Medicine at Mount Sinai, New York, NY, USA
[4] Department of Radiology, Hyogo College of Medicine, Hyogo, Japan
[5] Department of Medical Biochemistry, Academic Medical Centre, University of Amsterdam, Amsterdam, The Netherlands

Submitted: 03/08/2017. Revised: 22/09/2017. Accepted: 12/10/2017.

Corresponding Author:
Govindarajan Srimathveeravalli, Memorial Sloan Kettering Cancer Center, H112, 1275 York Ave, New York, NY 10065, USA.
Emails: srimaths@mskcc.org; reinert@mskcc.org

Table 1. Overview of Experimental Design With Details of Animal Assignments, Injection Timing, Sacrifice Time Point, and Assessment Techniques.

Sacrifice Time Point	Animal Numbers	Assessments	Tumor Location	Injection Details
6 hours	4 treated/4 untreated control	γ count, DOX measurement	Unilateral tumor	^{89}Zr-NRep/liposomal DOX (1 hour posttreatment)
24 hours	4 treated and 4 untreated control	γ count, DOX measurement	Unilateral=tumor	^{89}Zr-NRep/liposomal DOX (1 hour posttreatment)
48 hours	4 treated and 4 untreated control	γ count, DOX measurement	Unilateral tumor	^{89}Zr-NRep/liposomal DOX (1 hour posttreatment)
24 hours	3 treated/3 contralateral untreated control	PET imaging, autoradiography and histology	Bilateral tumor	^{89}Zr-NRep(injected 1 hour before treatment)
24 hours	3 treated/3 contralateral untreated control	PET Imaging, autoradiography and histology	Bilateral tumor	^{89}Zr-NRep(injected 1 hour after treatment)

Abbreviation: DOX, doxorubicin.

tumors drives selective uptake of systemically administered nanoparticles in tumors but not within normal tissue having intact microvasculature and functional lymphatic drainage. Electroporation-mediated rounding of endothelium and vascular lock could potentially alter the EPR effect of tumor vasculature, and their interaction has not been studied previously. Further, the cell membrane is permeabilized for a short duration during RE and barrier integrity typically recovers within a few minutes after pulse delivery.[14–15] The vascular effects however can last longer, and reports suggest them to persist up to 24 hours after RE.[5–9] As nanoparticles likely circulate longer than the time for which the membrane is permeabilized, the vascular effects of RE may also play a larger role in nanoparticle delivery to tumors.

Improved understanding of the diverse effects of RE is therefore crucial for designing optimal treatment regimens to deliver nanoparticle therapeutics such as liposomal doxorubicin (DOX) and albumin bound paclitaxel in patients. Pérez-Medina et al[16] previously validated ^{89}Zr-radiolabeled liposomal nanoparticle (^{89}Zr-NRep) as a positron emission tomography (PET) imaging reporter for monitoring the uptake of DOX in vivo. We hypothesize that effects of RE in vivo and RE-mediated DOX delivery can be monitored with ^{89}Zr-NRep. The objective of the present work was to use the ^{89}Zr-NRep to delineate the contribution of direct transfection and changes in vascular permeability during RE-mediated nanoparticle delivery and monitor the delivery of DOX in tumors.

Materials and Methods

Animal and Tumor Model

MiaPaca-2 cells were cultured using dulbecco's modified eagle medium modified to contain 1 mM sodium pyruvate, 1.5 g/L sodium bicarbonate and 4.5 g/L glucose, supplemented with 10% (vol/vol) heat-inactivated fetal calf serum and 100 IU penicillin and 100 μg/mL streptomycin. A total of 5 × 106 cells were then injected in athymic nude mice, strain NU(NCr)-Foxn1^{nu} (Charles River Laboratories, Wilmington, Massachusetts) in 150 μL of a 1:1 mixture of growth medium and Matrigel (Corning, Tewksbury, Massachusetts). Twenty-four animals were implanted with unilateral flank tumors, and 6 animals were implanted with bilateral flank tumors. Animals were selected for treatment when tumors reached 7 to 10 mm in size.

Radiotracer Preparation

The preparation of ^{89}Zr-labeled liposomes is described by Pérez-Medina et al.[17] Briefly, pegylated liposomes containing the phospholipid chelator Phosphatidylethanolamines-DFO were prepared by the sonication method. The DFO-bearing liposomes had a mean effective diameter (MED) of 105.8 ± 5 nm (polydispersity index [PDI] = 0.13 ± 0.02, n = 2) and a ζ-potential of −26.5 ± 5.4 mV (n = 1). ^{89}Zr-labeled liposomes had an MED of 119 ± 15 nm, PDI = 0.18 ± 0.08 (n = 2). Phospholipids for liposome preparation were purchased from Avanti Polar Lipids (Alabaster, Alabama). For radiolabeling, a solution of 0.3% DFO-bearing liposomes in phosphate buffered solution was reacted with ^{89}Zr-oxalate at 40°C for 2 hours, with final loading of 0.2 mCi/μmol total lipid content. The labeled liposomes were separated from free, unreacted ^{89}Zr through spin filtration.

Experimental Design and Treatment

The experiments were performed following guidelines in an Institutional Animal Care and Use Committee–approved protocol. Details of animal numbers, cohorts, sacrifice time point, and measurements performed in each cohort are provided in Table 1. Doxorubicin hydrochloride was purchased from Sigma-Aldrich (St Louis, Missouri), and pegylated liposomal doxorubicin (Doxil) was acquired from the hospital pharmacy. Mice with bilateral tumors were used to validate and monitor the effects of RE with ^{89}Zr-NRep and to identify relative contribution of direct transfection and vascular effects in the delivery of ^{89}Zr-NRep into tumors. Mice bearing unilateral tumors were used to determine the efficacy of RE for delivering DOX

to tumors and compare the uptake pattern of DOX with ^{89}Zr-NRep at 3 time points. Reversible electroporation was performed by placing two 21G stainless steel needles into the tumors. The needles were placed parallel to each other at a distance of 5 to 7 mm contingent on the size of the tumor, and calipers were used to guide placement. The length of the needle was insulated except for 5 mm at the tip that was left uncovered to allow the passage of electricity. Tumors were treated with pulses with sufficient voltage to induce an electric field with strength of 700 V/cm between the electrodes. Each animal was treated with 10 pulses delivered at 1 Hz with a pulse length of 90 μs. ECM835 generator (BTX, Harvard Apparatus, Holliston, Massachusetts) was used to deliver the square wave pulses. The pulse parameters were chosen for their ability to induce RE of the tumor with limited cytotoxic effects. Animals with bilateral tumors received treatment of only 1 tumor, and the contralateral side was kept as control. Mice with bilateral tumors received intravenous tail vein injection of the ^{89}Zr-NRep, either 1 hour before ($n = 3$) or after ($n = 3$) treatment. As cell membrane permeability during RE is limited 10 to 15 minutes in vivo,[12–13] delaying injection of ^{89}Zr-NRep 1 hour after pulse delivery is sufficient to isolate RE-related vascular effects from the direct transfection in the former cohort. All animals with unilateral tumors received intravenous tail vein injection of the ^{89}Zr-NRep (28.4 $\pm$ 0.4 μCi) and DOX (0.2 mg) 1 hour after pulse delivery. All animals were recovered posttreatment and were kept under regular observation until designated sacrifice time points based on the complete clearance of DOX and ^{89}Zr-NRep from blood pool.

Measurements and Imaging

Animals were sacrificed at time points as detailed in Table 1. Animals with bilateral tumors underwent PET imaging at 2 hours and 24 hours following injection of ^{89}Zr-NRep. Imaging was performed using an Inveon MicroPET/CT (Siemens Healthcare Global, USA). Whole body PET static scans recording a minimum of 50 million coincident events were performed, with duration of 10 to 20 minutes. The image data were normalized to correct for nonuniformity of response, dead time count losses, positron branching ratio, and physical decay to the time of injection, but attenuation, scatter, or partial volume averaging correction were not performed. The counting rates in the PET images were converted to equivalent activity concentration (percentage injected dose per gram of tissue) through the use of a system calibration factor. Images were analyzed using ASIPro VMTM software (Concorde Microsystems, USA). Quantification of activity concentration was done by averaging the maximum values in at least 5 regions of interest drawn on adjacent slices of the treated and untreated tumors. Tumors were excised and embedded in OCT (Sakura Finetek USA Inc, Torrance, California) and frozen and sectioned in 10-μm thick sections at 5 different levels throughout the tumor. Sections were imaged against a phosphor imaging plate (BASMS-2325; Fujifilm, Valhalla, New York), and the plates were read on a Typhoon 7000IP plate reader (GE Healthcare, Pittsburgh, Pennsylvania) at a pixel resolution of 25 μm. Postmortem, tumor samples from mice bearing unilateral tumors were carefully extracted and weighed. Tumors were then either divided into 2 to 3 smaller pieces or kept intact depending on the relative size of the tumor. The radiation in these tumor samples was counted using a Wizard 2480 Automatic Gamma Counter (Perkin Elmer, Waltham, Massachusetts). Quantification of DOX in the samples was performed as previously reported.[16] Immediately after γ counting, tumor samples were homogenized in lysis buffer (10:1 vol/wt ratio) and were processed for DOX extraction. Samples (200 μL) were added to a 96-well plate, and DOX measurements were performed using a microplate reader (Safire, Tecan, Männedorf, Switzerland). A calibration curve was generated by adding increasing known quantities of DOX to tumor sample lysates from untreated animals (no DOX or pulse delivery).

Histology

Tissue sections from animals bearing bilateral tumors (treated = 6, control = 6) underwent histology analysis. The OCT-embedded and sectioned frozen tumor samples were then stained with ionized calcium-binding adapter molecule 1 (IBA1) (microglia and macrophage marker), cleaved caspase-3, and hematoxylin and eosin (H&E). Stained slides were evaluated for signs of tumor necrosis or injury and to ascertain whether macrophage population played a role in nanoparticle uptake in treated tumors.

Statistics

Data were compiled, and descriptive statistical measures such as the mean and standard deviation were calculated. In animals with unilateral tumors, uptake of the ^{89}Zr-NRep and DOX between treated and untreated tumors was compared using the nonparametric Wilcoxon rank sum test at each time point (6, 24, and 48 hours posttreatment). The uptake behavior of ^{89}Zr-NRep and DOX was correlated by fitting a linear regression line. Data handling and statistical analysis were automated using software wherever possible (MatLab; MathWorks, Natick, Massachusetts).

Results

Reversible Electroporation–Mediated Membrane Permeabilization and Changes in Vascular Permeability Drive ^{89}Zr-NRep Uptake in Tumors

The presence of ^{89}Zr-NRep in the blood pool during pulse delivery resulted in immediate uptake of nanoparticles in EP-treated tumors as observed on PET imaging performed 2 hours postinjection (Figure 1A, white arrow; 10.57 $\pm$ 0.95% ID/g). Imaging at the same time point indicated the uptake of ^{89}Zr-NRep was limited in contralateral untreated tumors (Figure 1A, yellow arrow; 3.59 $\pm$ 0.45% ID/g) and in RE-treated tumors where ^{89}Zr-NRep was injected 1 hour after pulse delivery

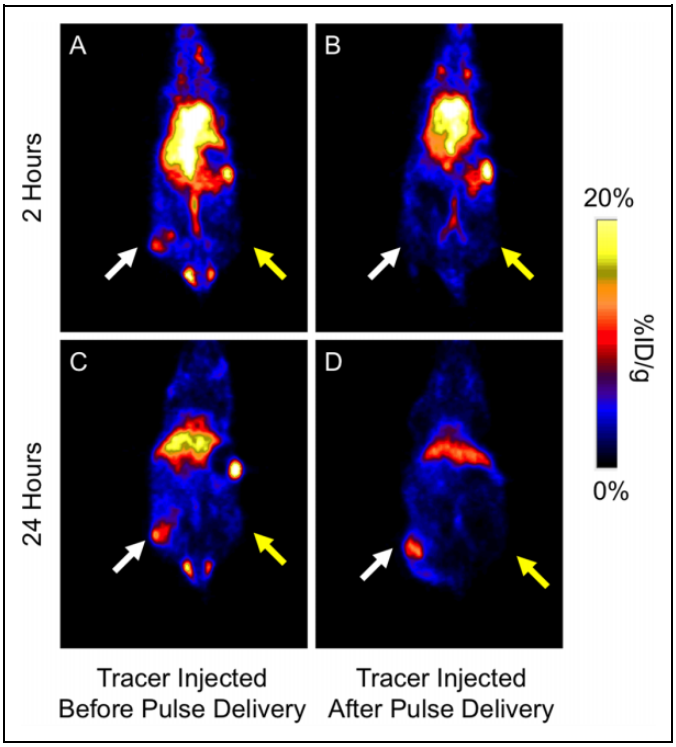

Figure 1. PET imaging suggests the uptake of ^{89}Zr-NRep at the 2-hour time point when injected before pulse delivery (A). Similar uptake cannot be seen when the ^{89}Zr-NRep was injected 1 hour following pulse delivery (B). However, 24 hours following treatment, there was no appreciable impact of injection/treatment order on the overall uptake (C and D). White arrows indicate tumors receiving treatment, and yellow arrows indicate contralateral untreated tumors. All images highlight the image slice demonstrating maximum uptake in the treated tumor.

(Figure 1B, white arrow; 6.61 $\pm$ 0.85% ID/g). However, PET imaging 24 hours following injection suggested uptake to be similar in tumors treated with RE after or before injection of ^{89}Zr-NRep (Figure 1C and D, white arrows), whereas contralateral untreated tumors (yellow arrows) demonstrated markedly lower levels of ^{89}Zr-NRep (inject/RE: 13.16 $\pm$ 0.69% ID/g vs RE/inject: 12.84 $\pm$ 7.18% ID/g vs contralateral control: 3.9 $\pm$ 1.3% ID/g; $P < .01$). Overall, when compared to untreated contralateral tumors, treatment with RE increased the deposition of ^{89}Zr-NRep in tumors, independent of the relative timing of tracer injection and pulse delivery. These findings were confirmed with postmortem autoradiography imaging of tumors (Figure 2A–C). Tumors undergoing RE exhibited insignificant tissue injury, which was limited to the immediate vicinity of needle placement (Figure 2D–E). Comparison of cleaved caspase-3 stains (Supplemental Figure 1) between RE treated and contralateral control tumors suggested small regions of increased staining adjacent to the location of needle placement, consistent with observations from H&E stains. Review of IBA1-stained samples did not indicate differences in the presence of macrophages in RE-treated and contralateral tumors, negating macrophages as the source of increased ^{89}Zr-NRep uptake.

Reversible Electroporation Accelerated Concentration of DOX But Does Not Increase Total Uptake

In mice with RE-treated tumors and mice held without RE, the maximum uptake of DOX was observed at 24 hours after injection. Levels of DOX in both RE-treated and untreated tumors gradually decreased at 48 hours after injection, suggesting utilization or clearance of DOX from the tumors (Figure 3, Table 2). When compared to tumors in untreated mice, tumors in RE-treated mice demonstrated accelerated DOX uptake 6 hours after injection. Measurements performed at the 6-hour time point indicated that treated tumors had 80.1% of their maximum measured DOX uptake, which was greater than untreated tumors that had just 30.6% of the maximum uptake at the same time point (Table 2). The differences in levels of DOX between RE-treated and untreated mice were not statistically significant at the 24- and 48-hour time points, suggesting that the RE-mediated increase in concentration of DOX did not persist at later time points. Despite a wide range in tumor weights and sizes included in the study, DOX uptake did not correlate with tumor mass in both RE-treated and untreated tumors (Figure 4). However, when compared to mouse with untreated tumors, the variation of DOX uptake in tumors was lower in the RE-treated cohort at the time point with maximum measured uptake (24-hour time point).

Reversible Electroporation–Mediated DOX Delivery Can Be Monitored With ^{89}Zr-NRep

^{89}Zr-NRep in tumors demonstrated a monotonous increase in both RE-treated and untreated tumors. Reversible electroporation–treated tumors had greater levels of ^{89}Zr-NRep at both 6- and 24-hour time points, but no significant difference was observed in overall uptake at 48 hours following injection (Table 2, Figure 3). Similar to trends observed with DOX, treatment with RE accelerated ^{89}Zr-NRep uptake. Measurements performed at the 6-hour time point indicated that RE-treated tumors had 78.8% of their maximum ^{89}Zr-NRep uptake (complete elimination from blood pool at 48 hours). In comparison, untreated tumors had just 41% of the maximum uptake at the same time point. Further, ^{89}Zr-NRep uptake did not exhibit any correlation with tumor size or mass in both treated or untreated tumors (Figure 4). The maximum uptake of DOX and ^{89}Zr-NRep was observed at 24 and 48 hours, respectively, suggesting ^{89}Zr-NRep was retained in tumors longer and not cleared in a fashion similar to DOX. Despite this discordance, there was no statistical difference between the uptake of ^{89}Zr-NRep and DOX at all time points. A high degree of correlation was observed between DOX and ^{89}Zr-NRep uptake in both RE-treated and untreated tumors (Figure 5) at all measurement time points.

Discussion

The results of this study demonstrates that companion imaging agents, such as the ^{89}Zr-NRep, can be used to monitor the

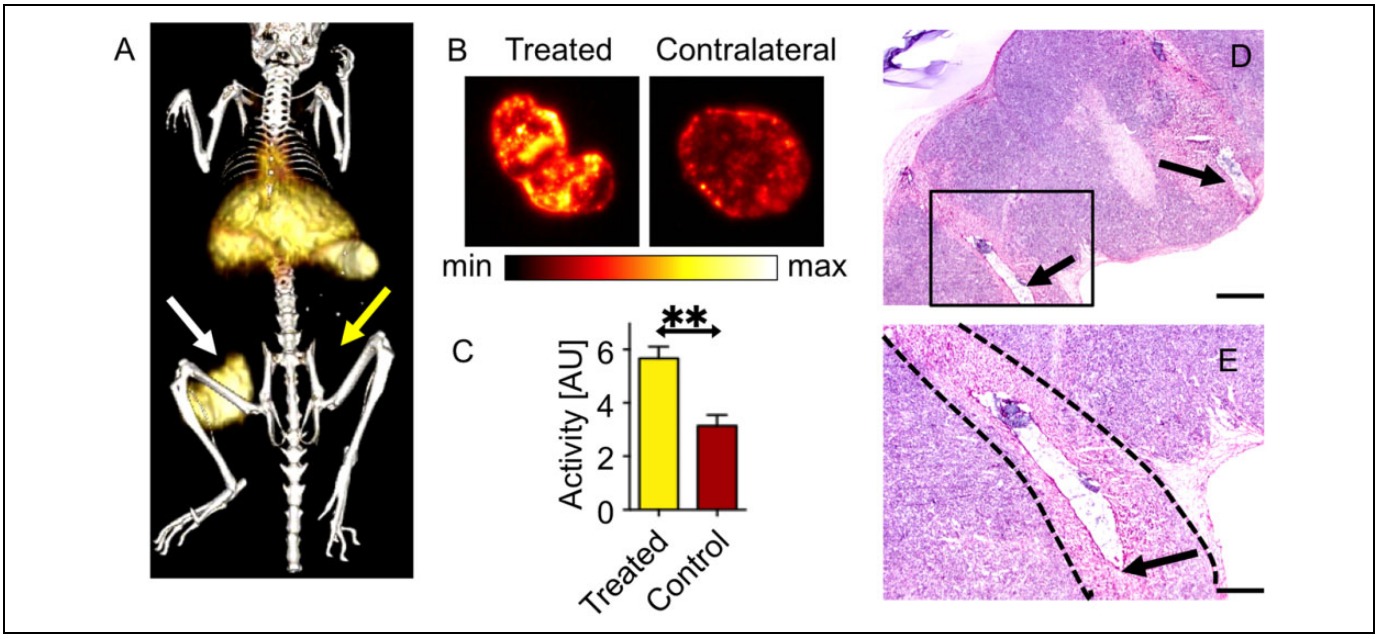

Figure 2. Isosurface of representing ^{89}Zr-NRep uptake in RE-treated tumor (white arrow) at 24 hours posttreatment, untreated tumor (yellow arrow) cannot be adequately visualized at the threshold value (A). Autoradiography of tumors treated with electric pulses (B) demonstrates the distribution of ^{89}Zr-NRep throughout the tumor. Graph of radiation counts comparing RE-treated tumors with contralateral control (C). Low magnification image (error bar = 1 mm) showing both needle tracts (arrows) and rectangle outline (D) is seen in higher magnification image (error bar = 0.5 mm) that shows region of necrosis (dashed boundary) closely bounded by defect in tumor from needle placement (arrow) (E). RE indicates reversible electroporation.

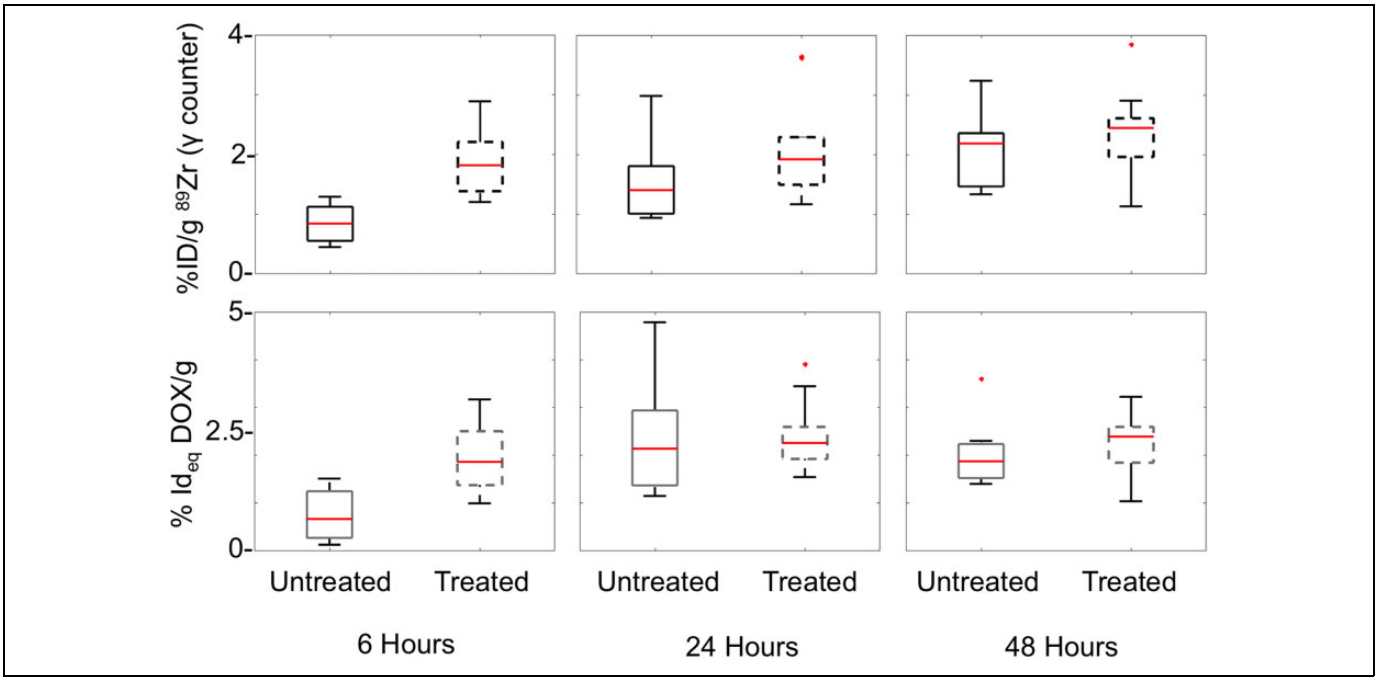

Figure 3. Uptake of ^{89}Zr-NRep and DOX in electric pulse treated and untreated tumors in mice bearing unilateral tumors, measured at sequential time points. Asterisk indicates data points which were more than 3 quartiles from the mean (outliers). DOX indicates doxorubicin.

effects of electroporation and predict RE-mediated uptake of nanoparticle therapeutics in vivo. ^{89}Zr-NRep used in this study has been previously validated as a companion-imaging agent for DOX and nanoparticle albumin bound paclitaxel.[16] In our study, uptake kinetics of ^{89}Zr-NRep and DOX were similar till 24 hours postinjection and then demonstrated slight divergence in uptake after 24 hours. This may be attributed to the breakdown and metabolization of DOX that was absent in

Table 2. Uptake of Liposomal Radiotracer (^{89}Zr-NRep) and the Liposomal DOX in RE-Treated and Control Mice with Unilateral Tumors.[a]

	^{89}Zr-NRep (mean [SD])			DOX (mean [SD])		
Cohorts	Treated (% ID/g)	Untreated (% ID/g)	P Value	Treated (% ID/g)	Untreated (% ID/g)	*P* Value
6 hours	1.86 (0.56)	0.84 (0.32)	$P = .003$	1.95 (0.76)	0.72 (0.55)	$P = .003$
24 hours	2.1 (0.87)	1.54 (0.72)	$P = .108$	2.41 (0.75)	2.35 (1.27)	$P = .6$
48 hours	2.35 (0.81)	2.06 (0.67)	$P = .35$	2.19 (0.67)	2.05 (0.75)	$P = .46$

Abbreviations: DOX, doxorubicin; RE, reversible electroporation; SD, standard deviation.
[a]Mean with standard deviation and confidence interval for different sacrifice time points.

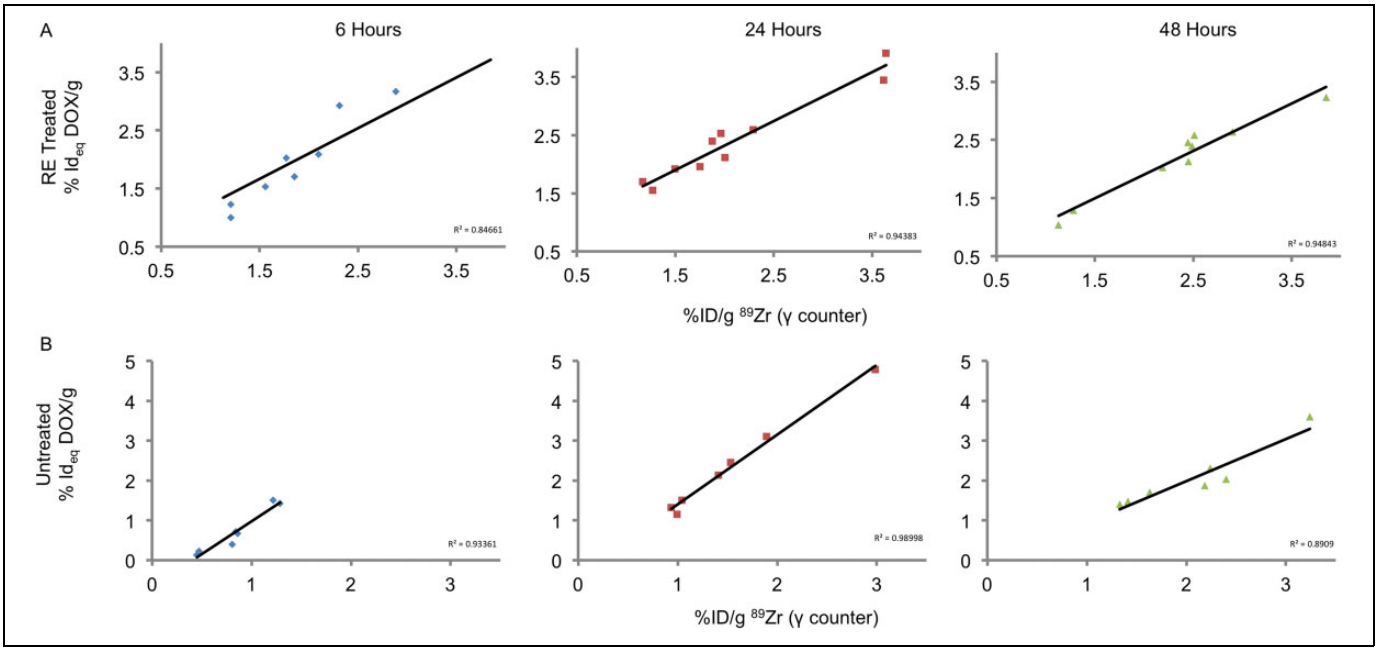

Figure 4. Correlation of ^{89}Zr-NRep and DOX uptake in mice with RE treated (top row) and mice with untreated tumors (bottom row) at sequential experimental time points. DOX indicates doxorubicin; RE, reversible electroporation.

^{89}Zr-NRep. Therefore, ^{89}Zr-NRep may be useful for monitoring early uptake behavior of DOX, but further comparison of uptake kinetics is required if the reporter is used to predict DOX uptake after 24 hours. Monitoring tissue effects of electroporation, such as membrane permeabilization and vascular changes, is difficult to accurately monitor with common imaging techniques. The SPIO[10–12] and radiolabeled nanoparticles[18] have been evaluated as contrast agents for imaging RE-mediated nanoparticle delivery with magnetic resonance imaging and PET imaging techniques. Our results extend these prior studies by demonstrating that companion imaging reporters can be used to monitor and predict DOX delivery using RE.

Membrane permeabilization has been considered the primary route for RE-mediated nanoparticle delivery into tumors. This assumption led to studies that closely timed the delivery of nanoparticles and electroporation[12] and used selective intra-arterial administration of nanoparticles to maximize the uptake following electroporation.[11,13] The results of our study identify that RE-related changes in vascular permeability could be another mode for delivery nanoparticles (DOX and ^{89}Zr-NRep) into tumors. Reversible electroporation–related changes in microvasculature are well-known to affect the transport of small and large molecules[5–9] into the treated tissue. These changes have been reported to increase the transport, or in some cases inhibit vascular flow, and the exact outcomes seem to be dependent on the tissue type, RE pulse parameters, and other factors. Comparison of the relative order of RE and ^{89}Zr-NRep injection suggests that injection of ^{89}Zr-NRep before pulse delivery elicited an immediate (2 hours post-RE) increase in ^{89}Zr-NRep uptake. However, measurements taken at the 24-hour time point demonstrated no differences in uptake between tumors from either group (injection before RE or injection after RE). This indicates that vascular effects of RE can play a major role in driving deposition of nanoparticles into tumors long after membrane permeability has recovered; this concept is described in Figure 6. Although ^{89}Zr-NRep remained in the blood pool for both cohorts, the lack of additional uptake in tumors treated after injection suggests there may be differences in nanoparticle washout from the tumor between the 2 groups, but the dynamics of washout is not

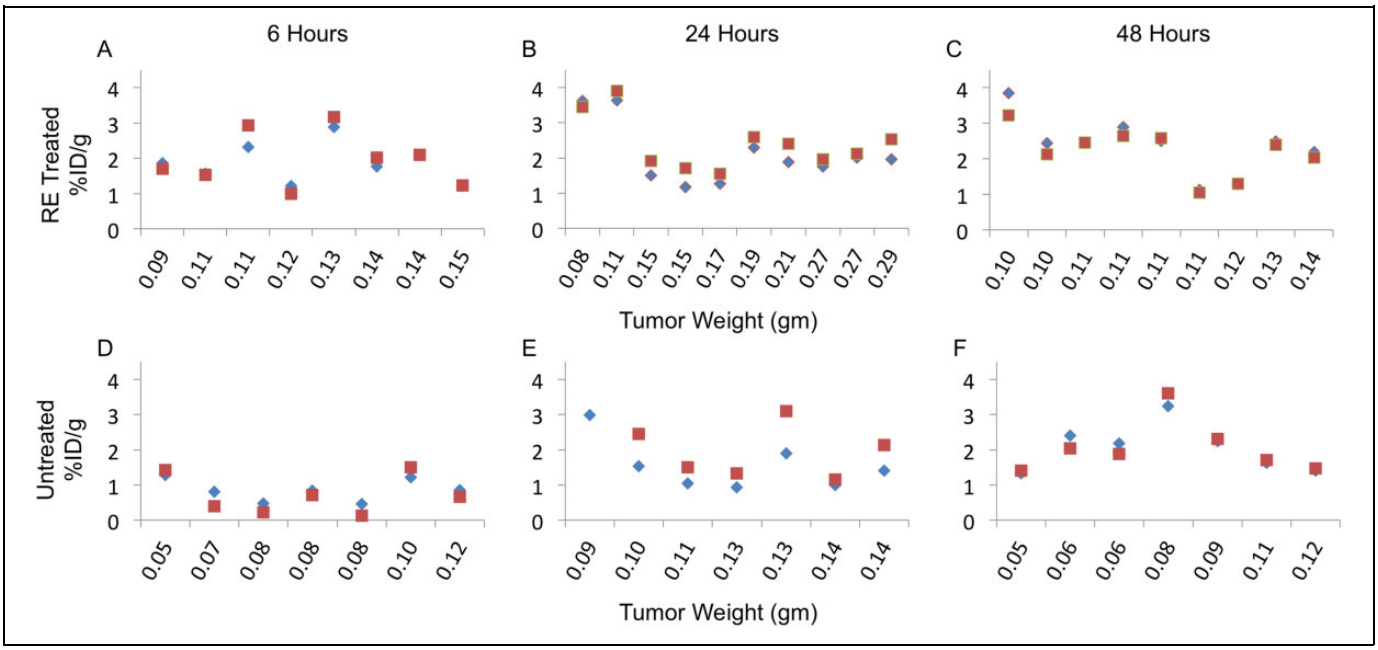

Figure 5. Comparison of ^{89}Zr-NRep (blue diamond) and DOX (red square) with tumor weight in RE-treated (A-C) and untreated (D-F) tumors. DOX indicates doxorubicin; RE, reversible electroporation.

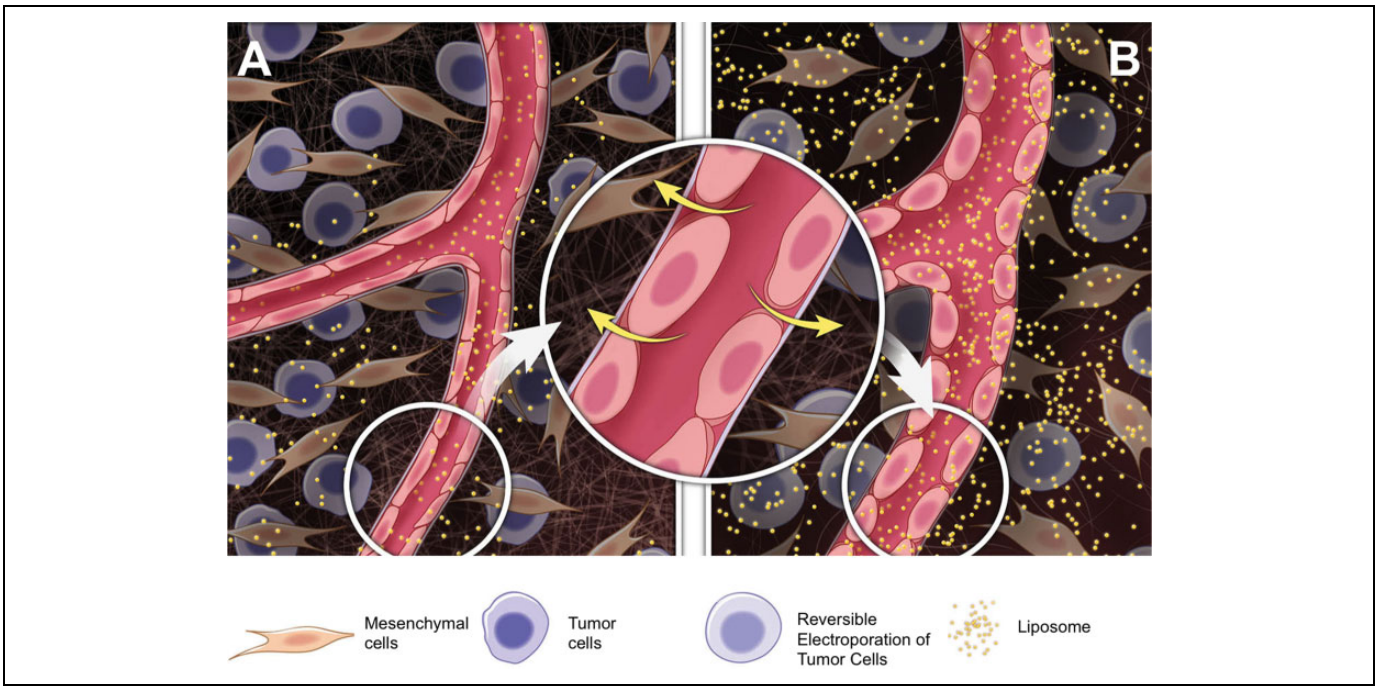

Figure 6. Schematic describing how RE-related vascular effects facilitates liposomal nanoparticle delivery. Compared to (A) untreated control tumors, (B) RE induces rounding of endothelial cells increasing penetration of the nanoparticles into treated tumors. RE indicates reversible electroporation.

apparent at this stage. Interestingly, tumor size or weight did not correlate with DOX or ^{89}Zr-NRep in both RE-treated and untreated tumors, indicating other biological factors (eg, vascular density) may underlie nanoparticle uptake. During electroporation, the cells are in a permeabilized state for a short window of time[14,15] within which the drug delivery is enhanced. Reversible electroporation–related changes in microvascular permeability could support decoupling delivery of electric pulses from injection of the therapeutic nanoparticle. The 2 effects offer contrasting benefits, where membrane permeabilization allows direct transfection of materials into the cell while vascular effects presumably deposit nanoparticles in

the tumor microenvironment. Therefore, the mode of electroporation-mediated nanoparticle delivery must be matched with the final goal of nanoparticle delivery.

Electroporation performed at higher energy settings yields 2 different treatment zones in tissue, an internal zone of cell death where the irreversible electroporation (IRE) occurs and an outer penumbra of RE. Studies evaluating nanoparticle uptake in combination with electroporation at high-energy settings hint at the presence of vascular effects. Unlike prior studies on RE, where particle uptake was immediate following injection/electroporation, Tam et al[18] demonstrated that maximum uptake of radiolabeled gold nanoparticles (30-50 nm) following IRE of liver tumors occurred 18 hours following delivery. Similar findings were also reported by Bulvik et al[19] who reported that treatment with IRE spared large blood vessels within liver tumors and increased vascular permeability. This effect increased the deposition of fluorescent polystyrene nanoparticles in treated regions, peaking at 24 hours following intravenous (tail vein) administration of the particles. The deposition of nanoparticles in the tumor was found to be independent of the size of the particle (20-500 nm).

Comparing nanoparticle accumulation following RE in bilateral and unilateral tumors indicates that the vascular effect of RE can accelerate nanoparticle deposition. Effectively, this can increase the concentration or dose of the therapeutic in a very short period of time. In the bilateral tumor model, faster ^{89}Zr-NRep deposition in RE-treated tumors led to competitive uptake when compared to untreated contralateral tumors. In turn, this led to 2- to 3-fold increase in nanoparticle uptake in treated tumors when compared to untreated controls. In unilateral tumors, this manifested as accelerated uptake in RE-treated tumors with maximum uptake being reached within 6 hours of treatment. In comparison, we estimate that in mice with untreated tumors the long circulation time ($\sim$48 hours) and slow clearance of DOX from the blood pool allowed the uptake in these tumors to catch up with that of RE-treated mice. From a therapeutic perspective, rapid accumulation of DOX in RE-treated tumors will increase the concentration of the drug within the tumor and may enhance the cytotoxic effect of such therapeutics. Also, RE is suited for the delivery of nanoparticles that clear rapidly (<24 hours) from the blood pool. It is possible that RE-mediated vascular effects wear off within 6 to 24 hours of pulse delivery, which needs to be validated with biodistribution studies. In addition, timing and delivery of nanoparticles need to be optimized to take advantage of electric pulse–mediated effects to increase the total uptake of particles. Taking findings from other studies to consideration,[11–13,18] intra-arterial nanoparticle delivery combined with RE can increase the overall uptake of nanoparticles. Another option would be to use active targeting, such as suggested by Luong et al[20] to promote binding of the nanoparticle once deposited into the tumor and improving retention. The use of nanoparticle with active targeting ligands may be more relevant when leveraging the vascular permeability effects for drug delivery than membrane permeabilization.

This study was performed with a single tumor model and therapeutic agent. At this point, it not clear whether similar outcomes for RE and ^{89}Zr-NRep will be seen in different tumor types. The study did not assess tumor necrosis or cell death in animals receiving RE-mediated DOX, limiting conclusions on the possible therapeutic benefits of RE-mediated DOX delivery. Further experiments are required to determine whether 24 hours represent the true time point for maximum uptake in RE-treated tumors or whether it occurs at an intermediary point between 6 and 24 hours.

In conclusion, results of this study demonstrate that the effect of RE on the vasculature plays an important role in nanoparticle delivery in tumors. ^{89}Zr-NRep has been validated to be a suitable imaging agent for both reliably monitoring the tissue effects of RE and also predict the uptake of DOX in RE-treated tumors. Reversible electroporation seems to accelerate the uptake of DOX and increase the concentration of drugs in treated tumors but may not increase the overall uptake of nanoparticles.

Acknowledgments

The authors thank the Small Animal Imaging Core, the Radiochemistry and Molecular Imaging Probes Core and the Molecular Cytology Core at Memorial Sloan Kettering Cancer Center for support.

Declaration of Conflicting Interests

The author(s) declared no potential conflicts of interest with respect to the research, authorship, and/or publication of this article.

Funding

The author(s) disclosed receipt of the following financial support for the research, authorship, and/or publication of this article: The authors acknowledge the support of NIH Cancer Center Support Grant (P30 CA008748) for core laboratory services that were used for the presented work. This work was supported by National Institutes of Health grants NIH 1 R01 HL125703 (W.J.M.), R01CA155432 (W.J.M.), R01CA204441 (T.R.), U54CA137788/ U54CA132378 (G.S), and the CNIC CardioImage program (C.P.M). The authors also thank the MSK Imaging and Radiation Sciences Program (for T.R.) for financial support.

Supplementary Materials

Supplementary material for this article is available online.

References

1. Gehl J. Electroporation: theory and methods, perspectives for drug delivery, gene therapy and research. *Acta Physiol Scand*. 2003;177(4):437–447.
2. Widera G, Austin M, Rabussay D, et al. Increased DNA vaccine delivery and immunogenicity by electroporation in vivo. *J Immunol*. 2000;164(9):4635–4640.
3. Wang L, Wang Z, Frank TG, Brown SI, Chudek SA, Cuschieri A. Rapid and efficient cell labeling with a MRI contrast agent by electroporation in the presence of protamine sulfate. *Nanomedicine (Lond)*. 2009;4(3):305–315.
4. Lin J, Chen R, Feng S, et al. Rapid delivery of silver nanoparticles into living cells by electroporation for surface-enhanced Raman spectroscopy. *Biosens Bioelectron*. 2009;25(2):388–394.

5. Sersa G, Cemazar M, Parkins CS, Chaplin DJ. Tumour blood flow changes induced by application of electric pulses. *Eur J Cancer*. 1999;35(4):672–677.
6. Markelc B, Bellard E, Sersa G, et al. In vivo molecular imaging and histological analysis of changes induced by electric pulses used for plasmid DNA electrotransfer to the skin: a study in a dorsal window chamber in mice. *J Membr Biol*. 2012;245(9):545–554.
7. Bellard E, Markelc B, Pelofy S, et al. Intravital microscopy at the single vessel level brings new insights of vascular modification mechanisms induced by electropermeabilization. *J Control Release*. 2012;163(3):396–403.
8. Sersa G, Jarm T, Kotnik T, et al. Vascular disrupting action of electroporation and electrochemotherapy with bleomycin in murine sarcoma. *Br J Cancer*. 2008;98(2):388–398.
9. Markelc B, Sersa G, Cemazar M. Differential mechanisms associated with vascular disrupting action of electrochemotherapy: intravital microscopy on the level of single normal and tumor blood vessels. *PLoS One*. 2013;8(3):e59557.
10. Zhang Z, Li W, Procissi D, Tyler P, Omary RA, Larson AC. Rapid dramatic alterations to the tumor microstructure in pancreatic cancer following irreversible electroporation ablation. *Nanomedicine (Lond)*. 2014;9(8):1181–1192.
11. Mouli SK, Tyler P, McDevitt JL, et al. Image-guided local delivery strategies enhance therapeutic nanoparticle uptake in solid tumors. *ACS Nano*. 2013;7(9):7724–7733.
12. West DL, White SB, Zhang Z, Larson AC, Omary RA. Assessment and optimization of electroporation-assisted tumoral nanoparticle uptake in a nude mouse model of pancreatic ductal adenocarcinoma. *Int J Nanomedicine*. 2014;9:4169–4176.
13. McDevitt JL, Mouli SK, Tyler PD, et al. MR imaging enables measurement of therapeutic nanoparticle uptake in rat N1-S1 liver tumors after nanoablation. *J Vasc Interv Radiol*. 2014;25(8): 1288–1294.
14. Saulis G. Pore disappearance in a cell after electroporation: theoretical simulation and comparison with experiments. *Biophys J*. 1997;73(3):1299–1309.
15. Levine ZA, Vernier PT. Life cycle of an electropore: field-dependent and field-independent steps in pore creation and annihilation. *J Membr Biol*. 2010;236(1):27–36.
16. Pérez-Medina C, Abdel-Atti D, Tang J, Zhao Y, et al.Nanoreporter PET predicts the efficacy of anti-cancer nanotherapy. *Nat Commun*. 2016;7:11838. doi:10.1038/ncomms11838.
17. Pérez-Medina C, Abdel-Atti D, Zhang Y, et al. A modular labeling strategy for in vivo PET and near-infrared fluorescence imaging of nanoparticle tumor targeting. *J Nucl Med*. 2014;55(10): 1706–1711.
18. Tam AL, Melancon MP, Abdelsalam M, et al. Imaging intratumoral nanoparticle uptake after combining nanoembolization with various ablative therapies in hepatic VX2 rabbit tumors. *J Biomed Nanotechnol*. 2016;12(2):296–307.
19. Bulvik BE, Rozenblum N, Gourevich S, et al. Irreversible electroporation versus radiofrequency ablation: a comparison of local and systemic effects in a small-animal model. *Radiology*. 2016; 280(2):413–424.
20. Luong D, Sau S, Kesharwani P, Iyer AK. Polyvalent folate-dendrimer-coated iron oxide theranostic nanoparticles for simultaneous magnetic resonance imaging and precise cancer=cell targeting. *Biomacromolecules*. 2017;18(4):1197–1209.